

Epitaxial neodymium-doped sapphire films, a new active medium for waveguide lasers

Raveen Kumaran,^{1,*} Scott E. Webster,¹ Shawn Penson,¹ Wei Li,¹ Thomas Tiedje,^{1,2}
Peng Wei,³ and Francois Schiettekatte³

¹Advanced Materials and Process Engineering Laboratory, University of British Columbia, Vancouver, British Columbia V6T 1Z4 Canada

²Currently with Department of Electrical and Computer Engineering, University of Victoria, Victoria, British Columbia V8W 2Y2 Canada

³Département de Physique, Université de Montréal, Montréal, Quebec H3C 3J7 Canada

*Corresponding author: raveen@phas.ubc.ca

Received June 12, 2009; accepted September 10, 2009;
posted October 1, 2009 (Doc. ID 112744); published October 27, 2009

Epitaxial films of neodymium-doped sapphire have been grown by molecular beam epitaxy on R-, A-, and M-plane sapphire substrates. The emission spectrum features sharp lines consistent with single-site doping of the Nd³⁺ ion into the host crystal. This material is believed to be a nonequilibrium phase, inaccessible by conventional high-temperature growth methods. Neodymium-doped sapphire has a promising lasing line at 1096 nm with an emission cross section of $11.9 \times 10^{-19} \text{ cm}^2$, similar to the 1064 nm line of Nd:YVO₄.

© 2009 Optical Society of America

OCIS codes: 160.5690, 160.3380, 310.0310.

Sapphire ($\alpha\text{-Al}_2\text{O}_3$) is an attractive laser host crystal because of its excellent thermomechanical properties and wide optical transparency. Solid-state lasers made from sapphire typically use transition metal dopants such as Ti or Cr, which are similar in size to the replaced Al ions. There are no reports of rare-earth-doped bulk sapphire crystals suitable for making lasers. It is likely that the equilibrium solubility of rare-earth ions in sapphire is very low at the melting point owing to the disparity in size between the small Al ions and large rare-earth ions.

Rare-earth-doped sapphire lasers would be better suited for power scaling, since the thermal conductivity of sapphire (33 W/m K) is large compared with other popular hosts such as YAG (11 W/m K) or YVO₄ (7 W/m K) [1,2]. While rare-earth-doped sapphire grown by bulk methods is unavailable, some progress has been made by using thin film techniques. Eu-doped sapphire grown by pulsed laser deposition produced distinct emission lines, but they were superimposed on broad peaks indicating the presence of other Al₂O₃ phases [3].

We report the growth of single-phase Nd-doped sapphire ($\alpha\text{-Al}_2\text{O}_3$) films on sapphire substrates by molecular beam epitaxy. The emission spectra feature sharp lines characteristic of Nd-doped crystal-line hosts, implying a uniform crystal field effect on the Nd³⁺ dopants. Among the emission lines, the 1096 nm line in the ${}^4F_{3/2} \rightarrow {}^4I_{11/2}$ manifold is dominant and a candidate for lasing action. Solid-state laser materials deposited in the form of thin films can be fabricated into planar waveguide lasers following methods borrowed from the semiconductor industry. These lasers have promising applications, such as the high-power sources in laser televisions [4].

Films were grown by using plasma-assisted molecular beam epitaxy with effusion cell sources for Al and Nd metal and a 300 W plasma source for generating active oxygen [5]. The background oxygen pressure during growth was 6×10^{-6} torr. The sapphire

substrates were furnace annealed in air at 1150°C for 8 h to generate ordered surfaces consisting of atomically flat terraces separated by atomic steps [5]. Nd-doped sapphire films up to 1 μm thick were grown between 400°C and 800°C at growth rates of 0.5–1 nm/min. The Nd doping level was up to 1 at. % relative to the Al concentration. The growth temperature is more than a factor of two below the melting temperature, thereby making it possible to fabricate nonequilibrium phases not accessible in growth from a melt. Films grown on R-, A-, and M-plane sapphire substrates were single crystal and followed the substrate orientation. Films grown on C-plane sapphire under similar growth conditions were found to be $\gamma\text{-Al}_2\text{O}_3$ (111). Emission from the $\gamma\text{-Al}_2\text{O}_3$ films was broad and resembled Nd:glass.

Among the Nd:sapphire films, thin (~ 100 nm) films with less than 1 nm rms surface roughness were grown between 400°C and 500°C. Figure 1 shows the x-ray diffraction characteristics of a 113-nm-thick film (107 nm Nd:sapphire on 6 nm sapphire buffer) grown on an A-plane sapphire substrate at 450°C. The Nd concentration, as measured by Rutherford backscattering spectrometry (RBS), is 2.35×10^{20} atoms/cm³ or 0.5 at. % relative to Al. The film has the same Nd concentration as 1.7 at. % Nd:YAG (based on the Nd/Y ratio), which is a suitable doping level for making lasers.

From the $\theta/2\theta$ scan in Fig. 1(b), the lower angle of the 0.5 at. % Nd:sapphire film peak corresponds to a 0.7% increase in vertical interplanar spacing. The spacing increases with Nd concentration, with a starting shift of 0.1% for undoped sapphire films. Due to the good crystalline quality and smooth surface of the film, x-ray thin film interference between the film and substrate led to the pendellösung fringes surrounding the film peak. The fringe spacing was used to verify the film thickness measured by RBS.

Figure 1(a) shows a reciprocal space map consisting of $\theta/2\theta$ scans with varying sample tilt ω . The film

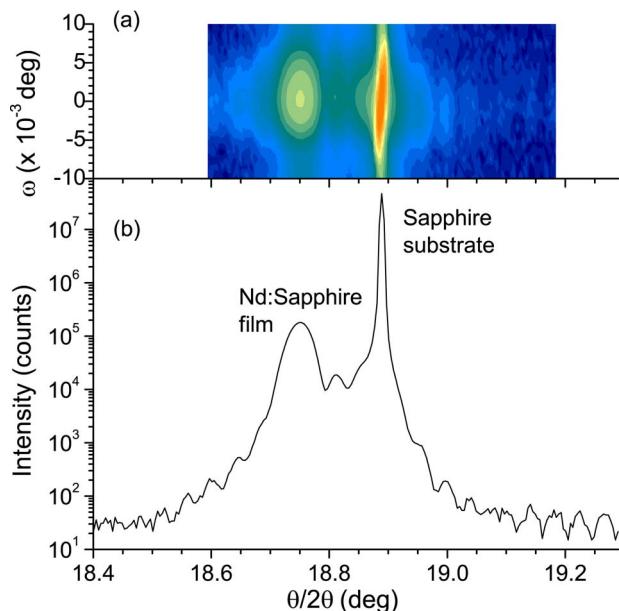


Fig. 1. (Color online) X-ray diffraction from a 107-nm-thick 0.5 at. % Nd:sapphire film grown on A-plane sapphire, showing (a) a reciprocal space map consisting of $\theta/2\theta$ scans for varying sample tilt ω and (b) a single $\theta/2\theta$ scan. The film peak is shifted to a lower angle from the substrate peak as a result of Nd doping. This shift increases with Nd concentration. Pendellösung fringes reflect the good overall structural quality of the film. The film thickness and Nd composition were measured by RBS.

and substrate peaks coincide in ω , indicating that the orientation of the crystal structure of the film matches the substrate. The FWHM of the film along ω is 23 arc sec.

Since sapphire is uniaxial, the emission spectrum is polarization dependent. In the case of the films deposited on M- or A-plane sapphire the optic axis is in the plane of the surface. The polarized emission from

a 1 μm M-plane Nd:sapphire film pumped with a 200 mW, 798 nm diode laser was passed through a calcite polarizer and measured by an InGaAs detector. The resolution of the measurement was 0.2 nm. The throughput of the optical system was calibrated by using a tungsten lamp.

The emission spectrum was used to calculate $\sigma\tau$, the product of emission cross section τ (not to be confused with the polarization) and lifetime τ , from the equation [6]

$$\sigma^{\text{pol}}(\lambda) \cdot \tau = \frac{3\lambda^5 I^{\text{pol}}(\lambda)}{8\pi c n^2} \left[\int (I^{\pi}(\lambda) + 2I^{\sigma}(\lambda)) \lambda d\lambda \right]^{-1}, \quad (1)$$

where n is the refractive index, I^{pol} is the polarized emission intensity, and pol is the polarization π or σ , which is parallel or perpendicular to the optic axis, respectively. The $\sigma\tau$ product is proportional to the gain efficiency and inversely proportional to the lasing threshold power. The dominant π -polarized line at 1096 nm has a $\sigma\tau$ product of $114 \times 10^{-24} \text{ cm}^2 \text{ s}$, comparable with that of Nd:YVO₄ ($100 \times 10^{-24} \text{ cm}^2 \text{ s}$) and almost twice that of Nd:YAG ($60 \times 10^{-24} \text{ cm}^2 \text{ s}$) at 1064 nm [7].

The lifetime was measured by using mechanically chopped pulses from a 1 W 514 nm Ar⁺ laser with emission collected by a photomultiplier tube. The time-resolved signal was current-amplified and monitored on an oscilloscope. A lifetime of 96 μs was measured for Nd:sapphire. Using this lifetime and the $\sigma\tau$ product, the emission cross section was obtained. Figure 2 shows the polarized emission cross sections for transitions from the $^4F_{3/2}$ manifold to the $^4I_{9/2}$, $^4I_{11/2}$, and $^4I_{13/2}$ manifolds. The π -polarized 1096 nm line has an emission cross section of $11.9 \times 10^{-19} \text{ cm}^2$,

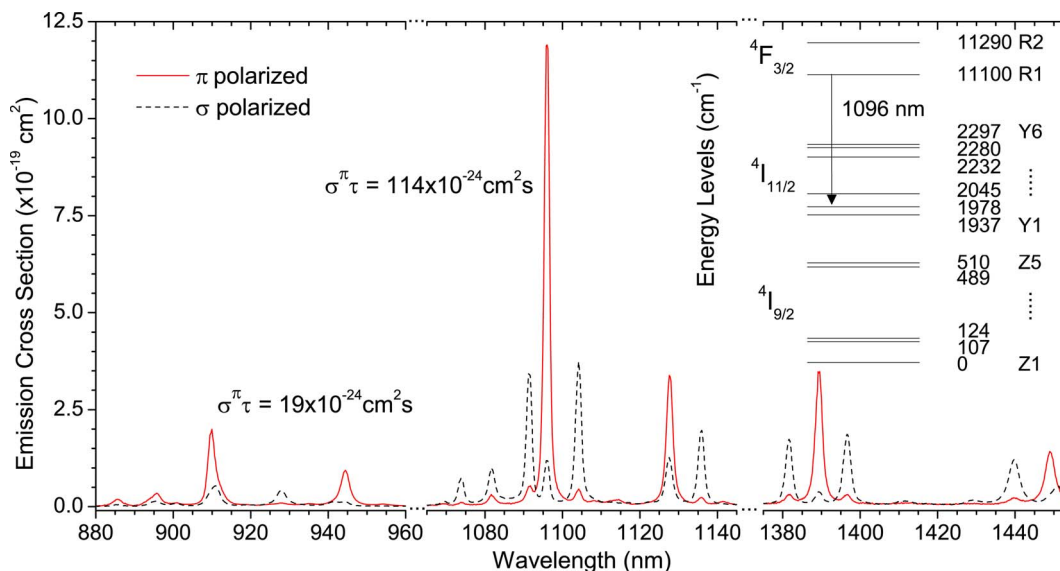


Fig. 2. (Color online) Room-temperature polarized emission cross sections of Nd:sapphire, showing transitions from the $^4F_{3/2}$ manifold to the $^4I_{9/2}$, $^4I_{11/2}$, and $^4I_{13/2}$ manifolds. π and σ polarizations occur when the electric field is parallel and perpendicular to the optic axis, respectively. $\sigma\tau$, the product of emission cross section σ (not to be confused with polarization) and upper state lifetime τ are listed for the strongest emission lines involving the $^4I_{9/2}$ and $^4I_{11/2}$ manifolds. Inset, room-temperature energy levels for the metastable as well as two lowest energy manifolds.

similar to Nd:YVO₄ ($13.5 \times 10^{-19} \text{ cm}^2$) and much larger than Nd:YAG ($2.6 \times 10^{-19} \text{ cm}^2$) at 1064 nm [7].

The inset of Fig. 2 shows the energy levels of the metastable as well as the two lowest energy manifolds. These levels were identified by using low-temperature (8 K) emission measurements to suppress transitions from the upper Stark energy level in the $^4F_{3/2}$ metastable manifold. The remaining transitions corresponded to the expected number of levels produced by the crystal field splitting of each Nd³⁺ multiplet.

Since the Nd:sapphire films are thin, direct-transmission-based absorption measurements were unsuccessful. Excitation spectroscopy was used instead, whereby a Ti:sapphire pump laser was manually tuned in nanometer increments and the integrated emission of the $^4F_{3/2} \rightarrow ^4F_{13/2}$ transition recorded. The Ti:sapphire pump was polarized along the optic axis of the Nd:sapphire crystal and calibrated for variations in power with changing wavelength.

As the product of absorption coefficient and thickness is small ($\ll 1$), the emission intensity, $I_{\text{emis}} = I_{\text{pump}} \eta (1 - \exp(-\alpha d)) \sim I_{\text{pump}} \eta \alpha d$ is proportional to the quantum efficiency η and absorption coefficient α . Assuming that η is constant, the π -polarized absorption spectrum of Nd:sapphire in the range 740–920 nm was obtained and is shown in Fig. 3. To approximately quantify the absorption strength, the reciprocity or McCumber method was used to relate the emission and absorption cross sections as shown by [8]

$$\sigma_a(\lambda) = \sigma_e(\lambda) \frac{Z_e}{Z_g} \exp \left[\left(\frac{hc}{\lambda} - E_{ZL} \right) / kT \right], \quad (2)$$

where σ_a and σ_e are the absorption and emission cross sections respectively, Z_e and Z_g are the partition

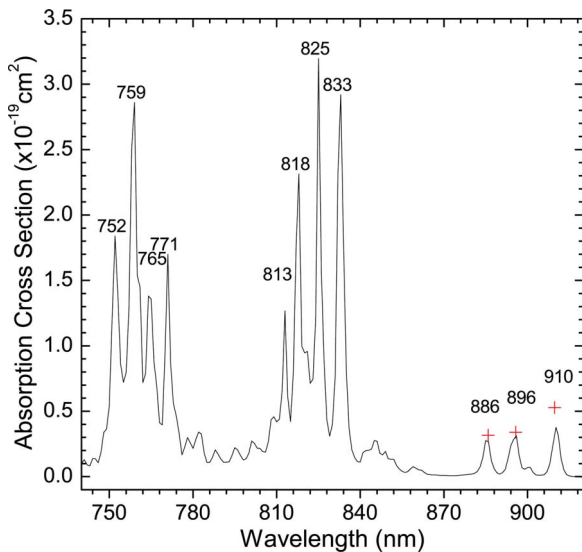


Fig. 3. (Color online) Room-temperature π -polarized absorption cross sections of Nd:sapphire measured by using excitation spectroscopy. Measurements were taken at 1 nm intervals. Peak wavelengths (in nanometers) are labeled. Crosses indicate fine measurements performed to obtain peak heights for use in the reciprocity relation, Eq. (2).

functions of the excited and ground manifold calculated from the energy levels in Fig. 2, and E_{ZL} is the energy level difference of the lowest levels in both manifolds.

Assuming no vibronic influence on the reciprocity, σ_a was calculated for three peaks in the $^4F_{3/2} \rightarrow ^4F_{3/2}$ transition of the π -polarized emission spectrum (Fig. 2). Since the absorption spectrum has only nanometer resolution, the heights of those three peaks were measured more accurately and are indicated by the crosses in Fig. 3. The scaling factors between the calculated σ_a and the three resolved absorption peaks were averaged and applied to the entire absorption spectrum. From the absorption data in Fig. 3, suitable laser pump wavelengths would be 825 or 833 nm with absorption cross sections of $\sim 3 \times 10^{-19} \text{ cm}^2$. This compares with $0.6 \times 10^{-19} \text{ cm}^2$ and $2.5 \times 10^{-19} \text{ cm}^2$ for Nd:YAG and Nd:YVO₄, respectively [9].

In conclusion, single crystal Nd-doped sapphire (α -Al₂O₃) thin films have been grown by molecular beam epitaxy on sapphire substrates. The narrow Nd emission lines indicate that the Nd ions are all located on sites with the same crystallographic symmetry, which we assume to be the Al site. We expect that the same growth method will also be applicable to sapphire doped with other rare-earth ions. The absence of reports in the literature of rare-earth-doped bulk sapphire suggests that the molecular beam epitaxy material is a nonequilibrium phase, inaccessible in growth from a melt. The strongest emission line in the Nd-doped material is at 1096 nm with a large emission cross section comparable with the 1064 nm line of Nd:YVO₄. This property, combined with the high thermal conductivity of sapphire, means that Nd:sapphire is an attractive candidate for the active medium in diode pumped waveguide lasers.

The authors thank NSERC for funding support and Dan Beaton and Georg Rieger for valuable discussions. Georg kindly provided access to a Ti:sapphire laser.

References

1. E. R. Dobrovinskaya, L. A. Lytvynov, and V. Pishchik, in *Sapphire: Materials, Manufacturing, Applications* (Springer, 2009), pp. 55–176.
2. J. Didierjean, E. Hérault, F. Balembois, and P. Georges, *Opt. Express* **16**, 8995 (2008).
3. G. Wang, O. Marty, C. Garapon, A. Pillonnet, and W. Zhang, *Appl. Phys. A* **79**, 1599 (2004).
4. Y. Hirano, S. Yamamoto, Y. Koyata, M. Imaki, M. Okano, T. Hamaguchi, A. Nakamura, T. Yagi, and T. Yanagisawa, in *Conference on Lasers and Electro-Optics* (Optical Society of America, 2008), paper CPDA3.
5. R. Kumaran, S. Webster, S. Penson, W. Li, and T. Tiedje, *J. Cryst. Growth* **311**, 2191 (2009).
6. P. F. Moulton, *J. Opt. Soc. Am. B* **3**, 125 (1986).
7. R. Moncorgé, in *Spectroscopic Properties of Rare Earths in Optical Materials*, G. Liu and B. Jacquier, eds. (Springer, 2005), pp. 320–378.
8. D. E. McCumber, *Phys. Rev.* **136**, A954 (1964).
9. Z. Huang, Y. Huang, Y. Chen, and Z. Luo, *J. Opt. Soc. Am. B* **22**, 2564 (2005).